International Journal of Advanced Engineering Application
Volume No.1 Issue No 7 Nov 2024
ISSN NO:3048-6807

Experimental Investigation of Convection Heat Transfer Performance Using CuO Nanofluid in Ethylene Glycol/Water Mixtures

[1]Brian Otieno,[2]Kevin Mwangi, [3] Daniel Kamau
[1,2,3]Department Of Mechanical Engineering
[1,2,3] Jomo Kenyatta University of Agriculture and Technology-Kenya

Abstract:

Technological advancements have necessitated efficient cooling solutions for electronic components, particularly central processing units. Water cooling systems, employing water blocks to transfer heat from components to circulating liquid, offer superior cooling compared to traditional methods, enabling higher performance and quieter operation. This study focuses on synthesizing nanofluids by dispersing CuO nanoparticles in water/ethylene glycol. Then, the nanofluids were tested as cooling liquids in computer water blocks to investigate their heat transfer properties and pumping power, aiming to assess their suitability for practical cooling applications. Experimental studies were conducted on CuO-ethylene glycol/water nanofluids, comprising CuO nanoparticles, 40% ethylene glycol as the base fluid, and 60% water by the total fluid volume. The tested nanoparticles volume fractions are 0.025%,0.055%, and 0.102%. The CuO-ethylene glycol/water nanofluid was prepared through sonication at 37 kHz for 3 hours. Subsequently, the nanofluids were tested on the water block with a flow rate ranging from 0.7 to 1.9 liters per minute. The results indicate that higher CuO concentration enhances heat transfer performance. However, it is worth noting that using higher nanoparticle concentrations may necessitate increased pumping power. This study provides valuable insights into the trade-offs between heat transfer and energy consumption for CuO-based nanofluids in electronic cooling system applications.

Keywords: Experimental study, CuO nanofluid, ethylene glycol, water mixture, convection heat transfer, heat transfer enhancement, thermal performance, nanotechnology, fluid dynamics

1. Introduction: The rapid advancement of technology has ushered in significant changes aimed at enhancing human efficiency across various tasks. This evolution has been paralleled by continuous developments in electronic equipment designed to support and augment human endeavors. As the demand for more efficient electronic devices grows, scientists are driven to create superior solutions, with computers as a prime example of this pursuit. Consequently, the widespread adoption of computers has surged with technological progress, spurring efforts to optimize their performance. A critical element in achieving effective computer performance is cooling the central processing unit (CPU), the computer's primary component. Efficient cooling is essential to ensure the quick dissipation of the CPU's heat, preventing overheating [1]. One common component for electronic cooling solutions is the heatsink, widely implemented on the CPU, power transistors, resistors, and other heat-dissipating components. Typically manufactured from materials such as aluminum or copper, heatsinks play a crucial role in facilitating heat transfer away from the electronic component, such as the processor in a computer. Advanced research on heatsink for thermal management in electronics have also been conducted by other investigators, including using unconventional materials like phase change material [2,3] and the study to find the most efficient cooling fluid flow configuration [4]. Various heatsinks have been deployed to fit specific needs and system arrangements, including heatsink casings, heatsink fans, water cooling systems (liquid coolers), and even dry ice coolers [5]. Among these, water cooling stands out as a noteworthy option for high-performance computing, which is employed to expedite electronic device cooling processes. This method uses a water block affixed to the critical, heatdissipating components. Water cooling boasts high efficiency and adaptability, as it permits adjustments to the shape and location of the cooling process without generating any disruptive noise, a drawback associated with traditional heatsink fans [6]. This has spurred ongoing research aimed at optimizing the application of water cooling systems to electronic devices, with the ultimate goal of achieving superior performance. At the heart of this system is the water block, a specialized device that leverages fluid flow to enhance heat transfer and accelerate the cooling of electronic components. The conducting base of the water block absorbs heat from the component, which is carried away by the

flowing liquid in the passage within the water block. The naming convention of water blocks corresponds to their specific liquid cooling process as a cooling medium [7].

Various liquid fluids can serve as cooling media, including water, oil, ethylene glycol, refrigerant, and nanofluid [8]. Nanofluid, characterized by its nanoparticle dispersion in a base fluid such as water, oil, ethylene glycol, or refrigerant, is a promising alternative for enhancing cooling performance due to its impressive thermal conductivity. Commonly utilized nanoparticles include CuO, Al_2O_3, TiO_2, among others. The nanofluid production process entails mixing the base fluid and nanoparticles under specific temperature and duration conditions, often facilitated by an ultrasonic cleaner employing vibrational frequencies to ensure thorough mixing [9]. Numerous studies have delved into the application of nanofluids as cooling media. For instance, Nuim Labib et al. [10] conducted an experiment examining heat transfer in forced convection within microchannels, employing Al_2O_3-water and CuO -water nanofluid mixtures. The study scrutinized the impact of varying nanofluid ratios on the heat transfer coefficient. The results underscored that CuO-water exhibited a significantly higher heat transfer coefficient than the base fluid, particularly when compared to the Al_2O_3 $^-$ water nanofluid. In more advanced research, a phase change material of PT-58 has been used in conjunction with graphene nanoplatelets and magnesium oxide nanoparticles, where the concentration of nanoparticles was reported to have a positive correlation with the cooling performance of the heat sink [11]. Heris et al. [12] researched heat transfer within a car radiator, utilizing a CuO nanofluid solution as the cooling medium and a base fluid composed of ethylene glycol and water. This investigation assessed the effects of incorporating nanofluids into a car's radiator, where an ethylene glycol/water mixture was traditionally used. The findings illuminated a substantial enhancement in heat transfer rates compared to conventional water-based fluids. The most favorable results were achieved using a 0.8vol% (CuO-ethylene glycol/water) nanofluid, resulting in an impressive 55% increase in the Nusselt value. These outcomes suggest that the Nusselt value escalates in response to increased flow rate, higher nanofluid concentration, and elevated radiator inlet temperature. In conclusion, the application of nanofluids proves highly effective in elevating heat transfer rates.

Our research group has studied the CuO nanofluid heat transfer characteristics within electronic device cooling systems. The study used nanoparticle volume fractions of $0.05\%, 0.32\%$, and 0.74% in a water-based fluid. The outcomes demonstrated the effectiveness of nanofluids in augmenting cooling, resulting in heightened temperature differences between the heater and the working fluid. Notably, the $0.32\%CuO$ concentration yielded the most substantial temperature difference at $13.71°C$, while the $0.74\%CuO$ variation exhibited the highest convection coefficient value at $588\ W/m^2\ °C$ [13]. Regarding nanofluid production, two primary methods exist: the one-step method and the two-step method. The one-step method simultaneously synthesizes and disperses nanoparticles within the base fluid, achieved through chemical processes or evaporation. In contrast, the two-step method involves separate nanoparticle synthesis and dispersion in the base fluid. The two-step method is more straightforward yet often leads to agglomeration; hence, additional stabilizing measures are required. The two-step method involves preparation techniques like sol-gel precipitation, spray pyrolysis, and high-energy milling (HEM), then mixing with base fluids using an ultrasonic cleaner. This method garners efficiency by capitalizing on vibrations during the mixing process. Nevertheless, the one-step method for nanofluid production boasts superior stability and nanoparticle dispersion compared to the two-step method [14].

In this study, the authors investigated the utilization of nanofluids as cooling fluids, using CuO nanoparticles with water and ethylene glycol as base fluids. Nanofluids were meticulously prepared by adding CuO nanoparticles to the base fluid of ethylene glycol and water, with volume fractions ranging from 0.1% to 0.5%. Notably, the nanoparticles were mixed for an extensive duration of 3 hours using an ultrasonic cleaner, a highly efficient method due to its ability to ensure comprehensive mixing within a shorter timeframe. Subsequently, these nanofluids were subjected to rigorous testing within computer cooling devices, primarily in the form of waterblocks. The main objective of this study is to reveal the potential of CuO nanofluid as a cooling liquid. While many published works on CuO nanofluids as coolants are of single base fluid, mostly water, we investigate using a hybrid base fluid that consists of water and ethylene glycol in a specific ratio. Within that framework, we report the production process and effect of the nanoparticle content on heat transfer characteristics and pumping power. This information serves as the basis for this type of nanofluid for specific real-case cooling solutions.

2. MATERIALS AND METHODS

Mixing nanofluids followed a one-step method, which involved preparing nanoparticles at concentrations of 0.1%, 0.3%, and 0.5%. These nanoparticles are then blended with a base fluid in a beaker, and the resulting mixture underwent a sonication process (exposure to ultrasonic waves) in an Elma S60 H-type ultrasonic cleaner [15]. The sonication process lasted 3 hours and employed ultrasonic waves with a frequency of 37 kHz [16]. After sonication, the nanofluids were

allowed to settle for 12 hours. Figure 1 illustrates the steps for creating nanofluids. The amount of nanoparticles and base fluid used depends on the desired volume fraction in the end product. We used volume fractions $0.1\%, 0.3\%$, and 0.5% [17] to make the mixture. The base fluid comprised 60% water and 40% ethylene glycol. The quantities of nanoparticles and base fluid for each volume fraction weighed with a digital scale with 0.01 g uncertainty are specified in Table 1 . Note that those percentages expressed in nanoparticle volume fractions $(0.1\%, 0.3\%, 0.5\%)$ are the initial quantities for the production process. As will be exhibited in the Results section, there are precipitates at the end of the mixing process. Thus, the actual fraction will be recalculated based on the net weight of nanoparticles dispersed in the solution by removing the precipitates that settle at the end of the mixing process. The actual percentages are stated in the Results section.

Subsequently, these nanofluids were experimented with in a commercial waterblock to determine their effectiveness as computer cooling fluids. The testing procedure adhered to the scheme outlined in Figure 2. The experiments of CuOethylene glycol/ water nanofluids were conducted with flow rates ranging from 0.7 to 1.9 liters per minute (lpm) at 0.3 lpm intervals. Temperatures were monitored and logged at the inlet of the waterblock, T_{in}, at the outlet, T_{out} , and at the surface of the heater, T_{heater} . Measurements were made using K-type thermocouples with 2.2°C uncertainty. As information for the interested readers to compare with other potential nanoparticles, the CuO nanoparticles have a 6500 kg/m^3 density and a heat transfer coefficient of $18\ \text{W/m.K}$ [18].

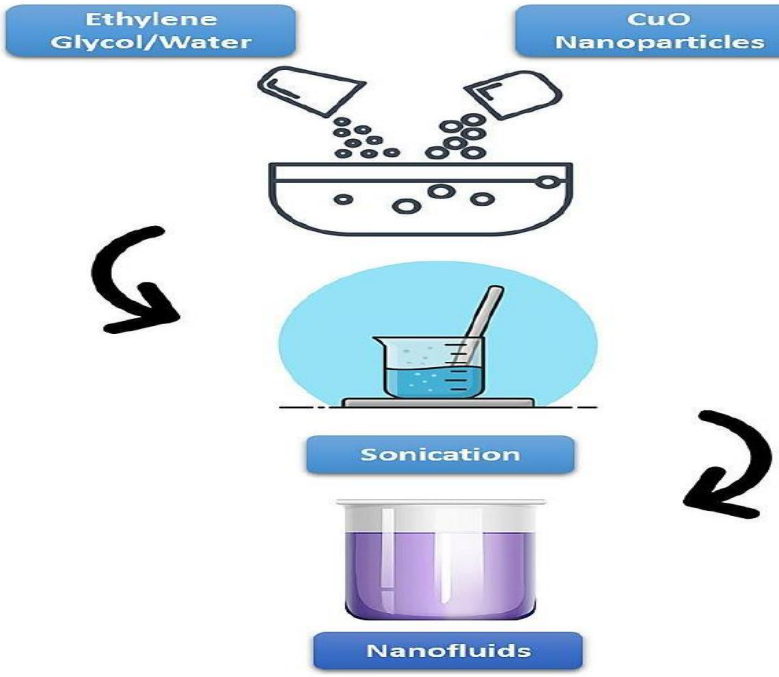

Figure 1. Nanofluids making stage

Table 1. Nanofluid composition

Composition	Nanoparticles (g)	Water (g)	Ethylene Glycol (g)
Water	0 ± 0.01	600.0 ± 0.01	400.0 ± 0.01
Water+Ethylene glycol + 0.1%CuO	3.79 ± 0.01	599.4 ± 0.01	399.6 ± 0.01
Water+Ethylene glycol + 0.3% CuO	11.36 ± 0.01	597.0 ± 0.01	398.0 ± 0.01

Water+Ethylene glycol +0.5%CuO	18.93 ± 0.01	594.0 ± 0.01	396.0 ± 0.01

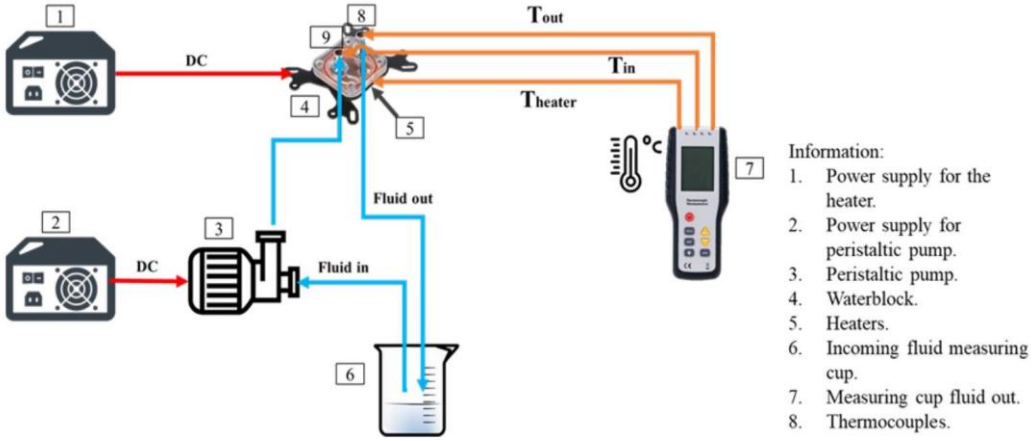

Figure 2. Scheme of nanofluid testing

3. RESULTS AND DISCUSSION

3.1 Physical and Visual Observation of the Synthesized Nanofluids

After sonication, precipitates exist at the bottom of the nanofluid containers (bottles) that are essentially insoluble nanoparticles that have not reached stable dispersion within the base fluid. Consequently, the precipitates were separated before using the nanofluids in the experimental cooling system setup. Since this separation removed some of the nanoparticles (precipitates) from the nanofluids, the stable solution and the precipitates were weighed to determine the net quantity of nanoparticles that had dissolved in the base fluid. The insoluble nanoparticles were dried before being weighed to ensure more accurate measurements.

Upon recalculation that excluded the precipitated nanoparticles, it was determined that the net nanoparticle weight fraction (NF) of 0.025% (NF 0.025%w/w) resulted from the initial mixture volume fraction of 0.1%; 0.055%(NF0.055% w/w) from the initial mixture of 0.3%; and 0.102%(NF0.102%w/w) from the initial mixture of 0.5%. Therefore, from this point onwards in this report, the nanofluids will be expressed in terms of the net content, i.e., 0.025%, 0.055%, and 0.102%. The images in Figure 3 depict the nanofluids contained in bottles after removing the precipitates, which can be considered stable nanofluids where the nanoparticles are uniformly dispersed. As outlined earlier, the readers should not refer to the percentage written on the label of each bottle in Figure 3 but instead to the recalculated net percentage stated in the caption of the corresponding image.

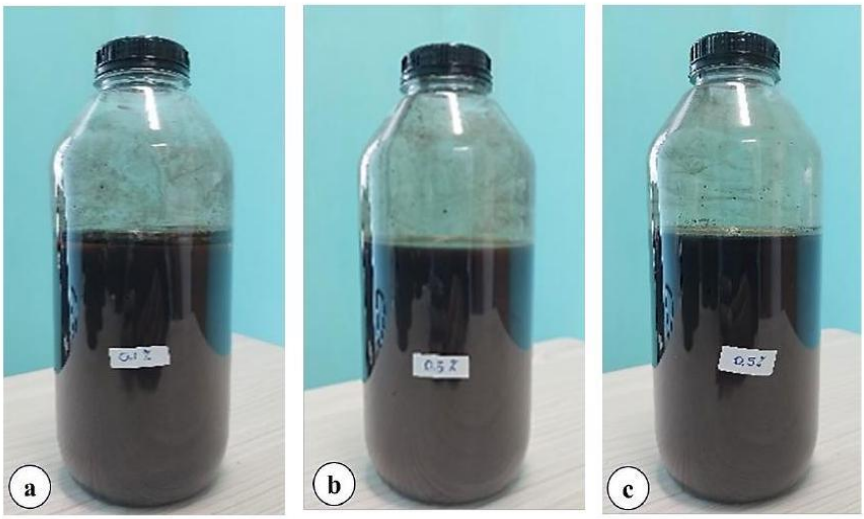

Figure 3. CuO nanofluid: (a) NF 0.025%, (b) NF 0.055%, and (c) NF 0.102%

3.2 Determining the Break-in Period for a Steady-State Analysis

Figure 4 illustrates a notable 1.3˚C drop in the heater temperature trend within the first 30 seconds of the cooling system operation. Although the temperature drop is lower than the uncertainty of the thermocouple itself, the trend is consistent to draw a convincing conclusion. This sudden decline at the beginning of the operation occurs because, during the experiment, the heater was turned on before the pump was. That being said, the heat accumulated while no cooling fluid flowed through the waterblock. Once the cooling fluid started to flow, a drop in the heater temperature became evident since the heat was rejected into the flowing fluid and carried away from the water block. After 30 seconds, there were no significant temperature fluctuations, and the heater temperature stabilized at around 54.1˚C, indicating that a steady-state condition has already been achieved.

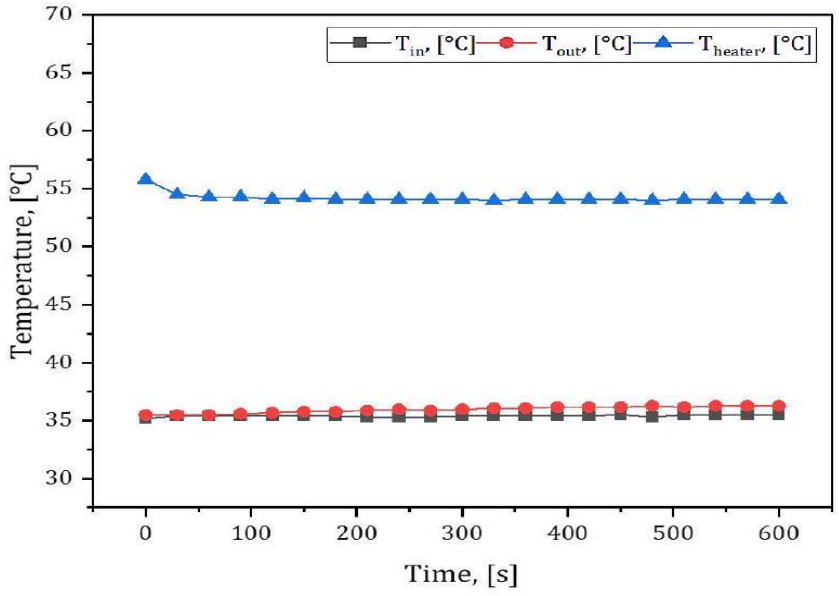

Figure 4. An example of temperature evolution at the initial period of the cooling system operation to determine the break-in period to reach steady-state condition, taken from the 0.102%CuO nanofluid at 1.3 lpm flow rate The inlet temperature reached stability only after 540 seconds, with an average inlet temperature of 35.4˚C. Understandably, the steady state condition of the inlet temperature (the nanofluid temperature at the inlet port of the water block) took longer because the system needed to heat the whole fluid in the loop. Similarly, the outlet temperature displayed a rise in the beginning of the cooling system operation until it reached steady state condition after 540 seconds

at 36.1°C. Note that the stability of both inlet and outlet temperatures occurs simultaneously. It makes sense because if the amount of heat supplied to the water block and the fluid flow rate are constant, as in our case, then the outlet temperature solely depends on the input one. This break-in period phenomenon, or initial regime before reaching steady-state condition, aligns with previous research conducted by Cao et al. [19], Vivek et al. [20], and Zakaria et al. [21]. By knowing that the steady-state condition has already been achieved after a certain period, the experiment can be conducted for repeatable results. In our case, the measurements after 600 seconds were utilized to calculate the convection coefficient and Reynolds number. As seen in Figure 5, and as discussed before, temperature readings have started to flatten out after 540 seconds; thus, 600 seconds is considered a safe point after which the steady state is guaranteed. This decision assumes that the values remained constant in the subsequent seconds, maintaining the steady-state condition.

3.2 The Effect of Flowrate Variations on Working Fluid Temperature

The difference in average working fluid temperature, $(T_{\text{in}} + T_{\text{out}})/2$, and heater temperature, T_{heater} for each experimented working fluid at different flowrate is plotted in Figure 5. Explicitly, this parameter is expressed as follows:

$$\Delta T = T_{\text{heater}} - [(T_{\text{in}} + T_{\text{out}})/2] \tag{1}$$

This parameter indirectly describes the heat transfer from the heater to the fluid. A larger value of ΔT infers that the working fluid has not significantly raised its temperature while passing through the heated region. In general, the fluid remains "cold"; hence, the difference in temperature from the heater is significant. It indicates that the fluid does not significantly absorb the heat generated by the heater as it flows through the water block. On the contrary, if a significant amount of heat is transferred into the working fluid, thus raising its temperature, then the difference between that fluid temperature and the heater will be less. That is reflected by the lower value of ΔT. Consequently, a lower ΔT is desirable in observing working fluid performance.

The results presented in Figure 5 indicate that water produces the highest temperature difference, whereas CuO nanofluid with a nanoparticle percentage of 0.102% (NF 0.102%) yields the lowest temperature difference. Ethylene glycol ranks second after water, followed by 0.025% and 0.055%CuO nanofluids. It can be summarized that higher nanoparticle content leads to superior heat transfer performance within the range of volume fraction tested in our experiments. This is attributed to the improvement of the heat transfer coefficient due to the presence of solid particles dispersed in the base fluid. CuO particles increase the fluid's conductive heat transfer component, which is commensurate with the concentration of those particles. This relation can be described via Maxwell relation in Eq. (2) [22]:

$$k_{nf} = k_b \frac{k_{np} + 2k_b + 2(k_{np} - k_b)\emptyset}{k_{np} + 2k_b - 2(k_{np} - k_b)\emptyset} \tag{2}$$

where, $\emptyset$ is the volume fraction given by Eq. (3), by knowing the volume concentration of nanoparticle, V_{np}, and of the base fluid, V_b.

$$\emptyset = \frac{V_{np}}{V_{np} + V_b} \tag{3}$$

Based on Eq. (2), it is evident that when the concentration of nanoparticle (represented by the volume fraction, $\emptyset$ increases, then the denominator will be reduced due to the negative sign of $-2(k_{np} - k_b)\emptyset$ term. In turn, the solution to k_{nf} will be higher. This equation is sufficient to explain the basic principle of the relation between nanoparticle concentration and heat transfer performance of the nanofluid. However, this work involves a sophisticated mixture comprising three components, water, ethylene glycol, and nanoparticles, in a non-ideal dispersion condition due to the variation of the nanoparticle sizes. Therefore, the effort to find the heat transfer coefficient is made based on experimental data, as elaborated in the ensuing section. Calculating and providing an exact figure of the parameters through the idealized formula, as in Eq. (2), instead, mislead and confuses the reader due to the substantial deviation. Nevertheless, the equation remains relevant to provide valid reasoning for the observed phenomenon.

As for the base fluids (ethylene glycol and water), ethylene glycol has a higher convective heat transfer coefficient than water, yielding better heat transfer performance, as the ΔT graph in Figure 5 reflects. Mixing these base fluids with ethylene glycol as the minor constituent improves the overall convective heat transfer without excessive cost impact by

keeping the low-cost material (water) as the major constituent of the mixture. The temperature difference decreases with an increase in the flow rate, as observed in the trend for each fluid variation. However, it's worth noting that the trend for water shows an increase between flow rates of 1 and 1.3 liters per minute (lpm) before decreasing again after flow rates exceed 1.3 lpm . Similarly, the trend for ethylene glycol indicates an increase in temperature at flow rates between 1 and 1.6 lpm . These temperature fluctuations may be attributed to the uncertainties in flow rate measurement at the specified values, leading to corresponding temperature increases or decreases.

The trend generally suggests that higher flow rates correlate with lower temperature differences. These findings align with previous research conducted by Zeng et al. [23] on testing the heat transfer capability of Al_2O_3-water in electronic cooling systems, as well as with Permanasari's research, which also demonstrated that an increase in flow rate led to an increase in the heat transfer coefficient value [24]. Similarly, the results of a study by Wengang et al. [25] revealed that an increase in air flow rate resulted in a decrease in the thermal resistance of the heatsink and an increase in the heat transfer rate.

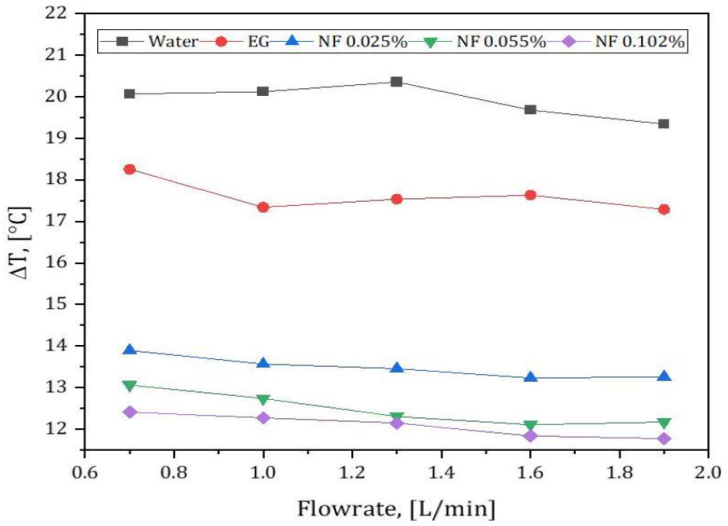

Figure 5. Effect of flowrate and concentration on the temperature difference of the heater and working fluid

3.3 Comparison of Convection Coefficients of Synthesized Nanofluids

The results obtained from various CuO nanofluid variations are presented in Figure 6. Water exhibits the lowest convection coefficient value, averaging 78.8 W/m^2 °C, while the highest convection coefficient value is achieved by CuO nanofluid with a volume fraction of 0.102%, averaging 147 W/m^2 °C. Nanofluids with a volume fraction of 0.055% rank second, with an average convective coefficient of 144 W/m^2 °C, followed by nanofluids with a volume fraction of 0.025% with 134 $W/m^{2.}$ °C. Ethylene glycol has an average convective coefficient value of 88.8 W/m^2 °C, as discussed before, which is higher than water. These findings align with previous studies conducted by Kumar et al. [26], Rafati et al. [27], and Shirzad et al. [28], all of whom noted that an increase in fluid concentration leads to an increase in the forced heat transfer coefficient value. Chabi et al. [29] research also demonstrated that the convection heat transfer coefficient increases with higher Reynolds numbers and nanofluid concentration. Again, it resonates with the Maxwell relation discussed in the preceding section.

Based on the convection coefficient values obtained from the three types of cooling fluids, CuO nanofluids exhibit superior heat transfer performance compared to using a single base fluid as a coolant, such as water or ethylene glycol. Figure 6 illustrates a significant difference in Reynolds values between ethylene glycol and nanofluid or water. Specifically, the Reynolds number for ethylene glycol ranges from 9 to 17 , while the Reynolds number for nanofluid and water ranges from 86 to 353 . This substantial difference is influenced by the disparity in viscosity values, with ethylene glycol having much higher viscosity than nanofluid and water [30]. Density values of the three cooling fluids also contribute to the differences in Reynolds values.

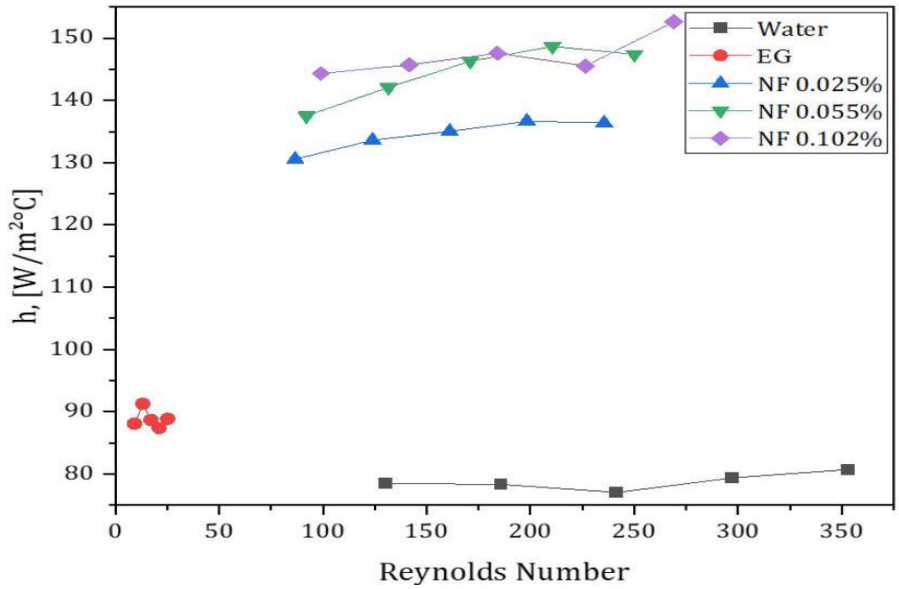

Figure 6. Relations of Reynolds number and convection coefficient

3.4 Analysis of Pumping Power

In Figure 7, it becomes evident that the pump power requirement escalates as flow rates increase. Equal flow rates were applied to all variations of cooling fluids to maintain consistency in assessing the pump power across different coolants. Water consistently exhibited the lowest demand for power across all specified flow rates, showcasing its efficiency as a coolant. On the other end of the spectrum, CuO nanofluid, with a volume fraction of 0.102%, was the most power-intensive working fluid, particularly at a flow rate of 1.9 lpm . Notably, the smallest pump power requirement was recorded for water, a mere 1.59 watts, while the largest was observed for CuO nanofluid with a volume fraction of 0.102%, peaking at 2.54 watts. Physically, the pumping power required for fluid circulation correlates directly with the applied flow rate, fluid viscosity, and density. Therefore, the power demand for maintaining fluid flow increases as flow rates increase. The higher viscosity and density impose greater resistance to flow, consequently necessitating more pump power to overcome these inertial loads [31].

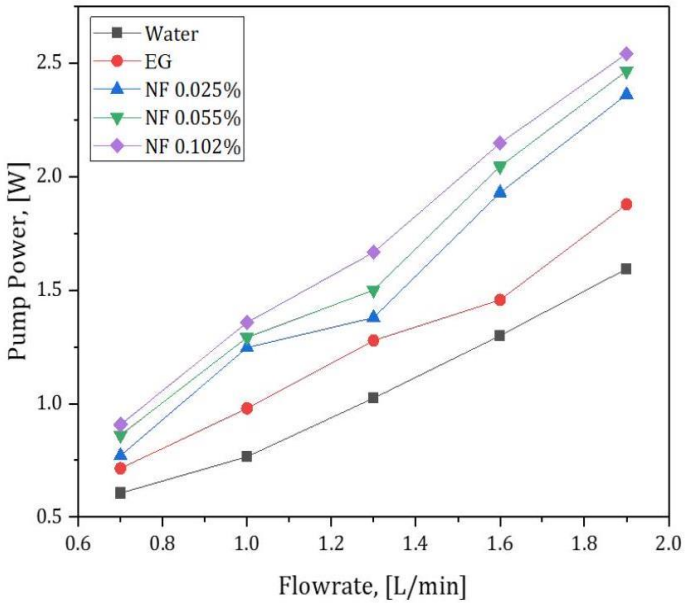

Figure 7. Relation of pumping power with flowrate of different working fluids

4. CONCLUSIONS

This study has shown the promising potential of CuO nanofluid as the working fluid in a liquid cooling system, particularly for electronic device cooling. The apparatus employed in this work are those commonly used in consumer electronics. Water and ethylene glycol are used as the base fluid, and the CuO nanoparticles are uniformly dispersed. Results demonstrated that within the weight fraction range tested in our experiments ($0.025\%w/w, 0.055\%w/w$, and $0.102\%w/w$), the heat transfer performance improvement positively correlates with increased CuO concentration. The convection coefficient of the produced nanofluid with $0.102\%w/w$ is about 95% higher than that of water. However, this excellent heat transfer performance comes at the expense of pumping power, where the top-performing nanofluid draws 40% more power than water. These findings provide valuable insights into the heat transfer characteristics and cooling efficiency of CuO -ethylene glycol/water nanofluids in the context of electronic device cooling systems.

REFERENCES

[1] M. W. Alam, S. Bhattacharyya, B. Souayeh, K. Dey, F. Hammami, M. Rahumi-Gorji, et al., "CPU heat sink cooling by triangular shape micro-pin-fin: Numerical study," International Communications in Heat and Mass Transfer, vol. 112, p. 104455, 2020.
[2] R. A. Lawag, H. M. Ali, M. H. Zahir, B. A. Qureshi, "Investigation of PT 58 and PEG-6000-based finned heat sinks for thermal management of electronics," Journal of Cleaner Production, vol. 390, p. 136101, 2023.
[3] T. Rehman, T. Ambreen, H. Niyas, P. Kanti, H. M. Ali, C. W. Park, "Experimental investigation on the performance of RT-44HC-nickel foam-based heat sinks for thermal management of electronic gadgets," International Journal of Heat and Mass Transfer, vol. 188, p. 122591, 2022.
[4] S. Saeed, A. Hussain, I. Ali, H. Shahid, H. M. Ali, "Thermal management of electronics to avoid fire using different air flow strategies," Fire, vol. 6, no. 3, p. 87, 2023.
[5] Intel, "CPU cooler: Liquid cooling vs. air cooling," California, 2024. [Online]. Available: https://www.intel.com/content/www/us/en/gaming/resources/cpu-cooler-liquid-cooling-vs-air-cooling.html
[6] G. Singh, M. Gupta, H. S. Gill, "Evaluating the cooling performance of light commercial vehicle with watercooled engine systems - An approach beyond regulatory standards," in Materials Today: Proceedings, vol. 48, pp. 1383-1389, 2021.
[7] B. P. Whelan, R. Kempers, A. J. Robinson, "A liquid-based system for CPU cooling implementing a jet array impingement waterblock and a tube array remote heat exchanger," Applied Thermal Engineering, vol. 39, pp. 8694, 2012.
[8] M. Salem Ahmed, M. R. A. Hady, G. Abdallah, "Experimental investigation on the performance of chilled-water air conditioning unit using alumina nanofluids," Thermal Science and Engineering Progress, vol. 5, pp. 589-596, 2018.
[9] M. K. Ramis, K. M. Yashawantha, A. Afzal, U. Faisal, "Effect of ultrasonication duration on stability of graphite nanofluids," International Journal of Mechanical and Production Engineering, vol. 6, pp. 61-64, 2018.
[10] M. Nuim Labib, M. J. Nine, H. Afrianto, H. Chung, H. Jeong, "Numerical investigation on effect of base fluids and hybrid nanofluid in forced convective heat transfer," International Journal of Thermal Sciences, vol. 71, pp. 163-171, 2013.
[11] F. Hassan, A. Hussain, F. Jamil, A. Arshad, H. M. Ali, "Passive cooling analysis of an electronic chipset using nanoparticles and metal-foam composite PCM: An experimental study," Energies (Basel), vol. 15, no. 22, pp. 8746, 2022.
[12] S. Z. Heris, M. Shokrgozar, S. Poorpharhang, M. Shanbedi, S. H. Noie, "Experimental study of heat transfer of a car radiator with CuO/ethylene glycol-water as a coolant," Journal of Dispersion Science and Technology, vol. 35, pp. 677-684, 2014.
[13] S. I. L. Gaol, "Testing the heat transfer characteristics of CuO nanofluids in electronic device cooling systems," Bachelor Thesis, Institut Teknologi Sumatera, Indonesia, 2021.
[14] S. Masoud Parsa, A. Yazdani, H. Aberoumand, Y. Farhadi, A. Ansari, S. Aberoumand, et al., "A critical analysis on the energy and exergy performance of photovoltaic/thermal (PV/T) system: The role of nanofluids stability and synthesizing method," Sustainable Energy Technologies and Assessments, vol. 51, p. 101887, 2022.
[15] A. Asadi, F. Pourfattah, I. M. Szilagyi, M. Afrand, G. Zyla, H. S. Ahn, et al., "Effect of sonication characteristics on stability, thermophysical properties, and heat transfer of nanofluids: A comprehensive review," Ultrasonics

Sonochemistry, vol. 58, p. 104701, 2019.
[16] K. M. Al-Araji, M. A. Almoussawi, K. J. Alwana, "The heat transfer performance of MWCNT, CuO, and Al_2O_3 nanofluids in an automotive engine radiator," E3S Web of Conferences, vol. 286, p. 01009, 2021.
[17] B. Sun, C. Peng, R. Zuo, D. Yang, H. Li, "Investigation on the flow and convective heat transfer characteristics of nanofluids in the plate heat exchanger," Experimental Thermal and Fluid Science, vol. 76, pp. 75-86. 2016.
[18] E. Abu-Nada, "Effects of variable viscosity and thermal conductivity of CuO-water nanofluid on heat transfer enhancement in natural convection: Mathematical model and simulation," Journal of Heat Transfer, vol. 132, no. 5, pp. 1-9, 2010.
[19] S. Cao, R. R. Rhinehart, "An efficient method for on-line identification of steady state," Journal of Process Control, vol. 5, pp. 363-374, 1995.
[20] V. I. Sharma, J. Buongiorno, T. J. McKrell, L. W. Hu, "Experimental investigation of transient critical heat flux of water-based zinc-oxide nanofluids," International Journal of Heat and Mass Transfer, vol. 61, no. 1, pp. 425431, 2013.
[21] I. A. Zakaria, W. A. N. W. Mohamed, M. B. Zailan, W. H. Azmi, "Experimental analysis of SiO_2-distilled water nanofluids in a polymer electrolyte membrane fuel cell parallel channel cooling plate," International Journal of Hydrogen Energy, vol. 44, no. 47, pp. 25850-25862. 2019.
[22] A. Y. M. Ali, A. H. El-Shazly, M. F. El-Kady, S. E. Abdelhafez, "Evaluation of surfactants on thermo-physical properties of Magnesia-oil nanofluid," in Materials Science Forum, vol. 928, pp. 106-112, 2018.
[23] S. Zeng, P. S. Lee, "Topology optimization of liquid-cooled microchannel heat sinks: An experimental and numerical study," International Journal of Heat and Mass Transfer, vol. 142, p. 118401, 2019.
[24] A. A. Permanasari, B. S. Kuncara, P. Puspitasari, S. Sukarni, T. L. Ginta, W. Irdianto, "Convective heat transfer characteristics of TiO2-EG nanofluid as coolant fluid in heat exchanger," in AIP Conference Proceedings", p. 050015, 2019.
[25] H. Wengang, W. Lulu, Z. Zongmin, L. Yanhua, L. Mingxin, "Research on simulation and experimental of thermal performance of LED array heat sink," in Procedia Engineering, vol. 205, pp. 2084-2091, 2017.
[26] V. Kumar, J. Sarkar, "Particle ratio optimization of Al_2O_3-MWCNT hybrid nanofluid in minichannel heat sink for best hydrothermal performance," Applied Thermal Engineering, vol. 165, p. 114546, 2020.
[27] M. Rafati, A. A. Hamidi, M. Shariati Niaser, "Application of nanofluids in computer cooling systems (heat transfer performance of nanofluids)," Applied Thermal Engineering, vol. 45-46, pp. 9-14, 2012.
[28] M. Shirzad, S. S. M. Ajarostaghi, M. A. Delavar, K. Sedighi, "Improve the thermal performance of the pillow plate heat exchanger by using nanofluid: Numerical simulation," Advanced Powder Technology, vol. 30, no. 7, pp. 1356-1365, 2019.
[29] A. R. Chabi, S. Zarrinabadi, S. M. Peyghambarzadeh, S. H. Hashemabadi, M. Salimi, "Local convective heat transfer coefficient and friction factor of $CuO/$ water nanofluid in a microchannel heat sink," Heat and Mass Transfer, vol. 53, no. 2, pp. 661-671, 2017.
[30] R. S. Khedkar, N. Shrivastava, S. S. Sonawane, K. L. Wasewar, "Experimental investigations and theoretical determination of thermal conductivity and viscosity of TiO2-ethylene glycol nanofluid," International Communications in Heat and Mass Transfer, vol. 73, pp. 54-61, 2016.
[31] A. A. A. Abdullah Alrashed, O. A. Akbari, A. Heydari, D. Toghraie, M. Zarringhalam, G. A. S Shabani, et al., "The numerical modeling of water/FMWCNT nanofluid flow and heat transfer in a backward-facing contracting channel," Physica B: Condensed Matter, vol. 537, pp. 176-183, 2018.